Raman Spectroscopy using a Concatenated Laser System to Measure Water Content and Chemicals in Fuel

Tyler Morris, Yaelle Olivier

Dept. of Electrical Engineering and Computer Science,
College of Optics and Photonics
The University of Central Florida, Orlando, Florida, 32816

***ABSTRACT* — THE objective of this project is to identify and test water content in fuel, in this case, biofuel or biodiesel through a Raman spectroscopy and concatenated laser system. The solution is expected to improve accuracy and efficiency for testing, especially for large gas and oil companies. Our group chose this project as our senior design project because we feel we can provide a good mix of optics and photonics and computer engineering skills to formulate a solution for the detection of water content contamination.**

I. Introduction

Fuel is still an extremely reliable source of power especially in natural disasters and for heavy machinery. With this said the number one reason for equipment failure in natural disaster relief programs is due to bad fuel. This is not because the fuel is bad or unreliable, but because this gasoline or diesel is from emergency storage tanks that are often not checked regularly or before use in a natural disaster situation. When storage tanks that contain fuel go unchecked, they can start to collect water, and eventually that water will develop bacteria which will feed off the fossil fuels creating clusters called sludge. This water contamination is the first step in causing bacteria and other growths in the fuel to make it unusable.

In today's market, there are kits for detecting water contamination or bacterial growth in the fuel. However, these kits either use chemical reactions with the fuel and/or take a long time for the results. Many of these are also based on a qualitative measurement such as color or physical separation of the mixture. We think there could be a more effective way to measure fuel quantitatively in a short amount of time without using chemicals. This is where we would use optical technology and machine learning to do so, by use of Raman Spectroscopy using a Concatenated Laser system (RSCL). This system can detect water content among other substances and chemicals by using a Raman spectroscopy setup with two lasers rather than the typical one laser system. There are Raman spectroscopy systems already created to find chemicals in fuel, however, there is only proof of one current Raman probe that uses a dual-wavelength system and that is Innovative Photonic Solutions (IPS). They hold the patent for the probe.

The RSCL will be portable and easy to use within minutes, for quick fuel analyzations on the spot in the field. It will be made with the user and safety in mind, whether the user is a technician or an engineer. Looking further on, the RSCL can be used for more purposes than just fuel. It could be accommodated to find water in different chemicals and substances.

II. RSCL Profile

A. Objective Description

Through Raman spectroscopy we can find a chemical fingerprint of the sample by the wavelengths it emits without damaging the sample. Raman spectroscopy has already been used to find the chemical fingerprint of fuel through a single laser system. This provided a way to correctly characterize and quantify the adulterant and chemical compositions in fuel. Usually, quality control on fuel is done by measuring the physical properties like density, vapor pressure, and boiling points rather than accurate chemical characterizations. It has been tested and proven that Raman Spectroscopy with a laser (785 nm) was able to and quantify the adulterant in each fuel sample with low errors. Water concentration can be measured with the Raman system by expanding the measurement spectral range into molecular stretch regions. To do this we must add a second laser system (680 nm) to see spectral regions where stretch regions are prevalent. We then Raman shift and concatenate the data from both wavelength spectrums. So, there is a clear fingerprint region (785 nm) and a stretch region (680 nm). Not to mention, we can also do this in reverse, we can use this same system to detect fuel contamination in water sources.

As of the date of this paper, Innovative Photonic Solutions (IPS) has a patent out on a Raman probe that uses concatenated lasers. Under the patent, they are using dual-wavelength Raman probe byways of two laser sources. One of the excitation wavelengths is used for Raman scattering in the fingerprint region and the other has an excitation wavelength causing scattering in the stretch region. This is very similar to the RSCL however this is for a Raman probe whereas we are creating a Raman subsystem where a vial of the sample will be dropped into the system. This RSCL is not just the optical Raman subsystem but it also contains the integration of an algorithm in the computer to tell you what you're looking

at spectra-wise, whether the amount of water detected in the fuel is dangerous or not.

B. *Raman Spectroscopy*

In Raman spectroscopy we see virtual energy states, so we see Rayleigh, stokes, and anti-stokes scattering. Rayleigh scatter has no exchange of energy, so the incident light and scattered photons are the same wavelength or frequency. Stokes's scattering is when the atom virtually absorbs the energy, and the scattered photon has less energy when emitting a wavelength than the incident photon. The anti-Stokes scattering happens when the scattered photon has more energy than the incident photon. As said previously the Rayleigh is usually ignored and canceled out by filters and the anti-Stokes are usually very weak and ignored as well. It is important to note that this vibrational energy that happens during Raman spectroscopy is not the same as a laser exciting a molecule. When using a Raman system, the wavelengths or wavenumbers are usually shifted according to the excitation laser. This also means that the scattered light collected from a sample is not as frequent as absorption spectroscopy, the scattered light used for Raman through vibrational spectroscopy is about 1 in 10,000 photons. To make it possible to see these infrequent photons we set the integration time of the spectrometer to be longer allowing more light in as well as using a more powerful laser. However, when doing this one can saturate the laser with the incident wavelengths, to avoid saturation we add in optical filters throughout the system.

For Raman shift as seen in equation (1) is usually reported in wavenumber and wavelength are inverses of each other. In the optics community, we use wavelength while in the chemistry community they use wavenumbers. A wavenumber is just 1/ λ usually in cm^{-1}.

$$\Delta\tilde{\nu} = \left(\frac{1}{\lambda_0} - \frac{1}{\lambda_1}\right) \quad (1)$$

Where the $\Delta\tilde{\nu}$ is the Raman shift, λ_0 is the excitation wavelength, and λ_1 is the Raman spectra wavelength.

C. *Dual-wavelength laser*

As explained in the topic previous, usually we use a single excitation laser for a Raman Spectroscopy system but often these measurements will suffer from fluorescence. For Raman scattering the name of the game is to avoid fluorescence as much as possible, therefore near-infrared is preferred, as fewer molecules absorb near-infrared light especially compared to the visible region. That's the reason we are using a 785 nm wavelength laser for the fingerprint region because it provides a high Raman intensity and considerably low fluoresces. Our excitation wavelength of 785 nm the wavenumber range will go from 0-2000 cm^{-1} . With fluoresce however it makes it difficult to see the "stretch region" in the spectra in the range of 2000-4000 cm^{-1}. That is why we can integrate a second laser with a shorter wavelength and higher photon energy to collect the stretch region as seen in the figure below. For this, we want a second laser that is about 2000 cm^{-1} away from the first wavelength like a 680 nm laser. The lasers are going through the same fiber and virtually hitting the same spot on the sample. Using the spectrometer to collect data from each wavelength we then concatenate the data together which will show an increased peak/ peaks in the stretch region. This has been used before and is patented by IPS (Innovative Photonic Solutions). However, it is patented for a Raman Probe. We can learn a lot from this moving forward and understanding exactly what each wavelength does.

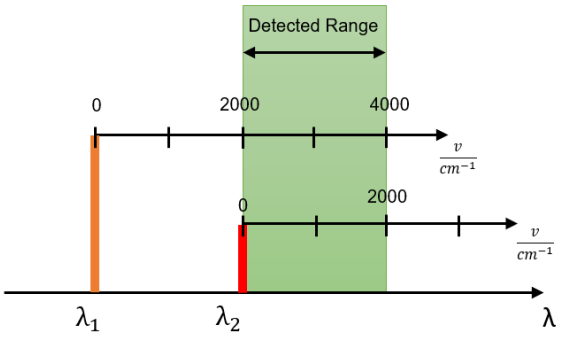

Through the testing process, we were able to see what we were looking for with both incident wavelengths as seen in the image below. We have samples at 0%, 25%, 50%, 75%, and 100% water in biofuel. In the first section of the Raman shifted graph, we see the fingerprint region which is our 785 nm laser. Each of these peaks corresponds to a certain chemical fingerprint that makes up the biofuel. We then move onto the middle section where we see our last peak in the fingerprint region is small, but it matches up perfectly with the first peaks of the stretch region. Right after this peak, we see our water peaks. The water peaks are seen in the stretch region using a 680 nm incident wavelength because we are seeing the physical stretch of the molecules, we don't see this in the fingerprint region because it is not Raman responsive.

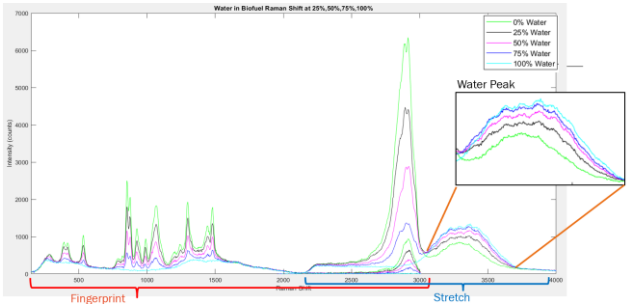

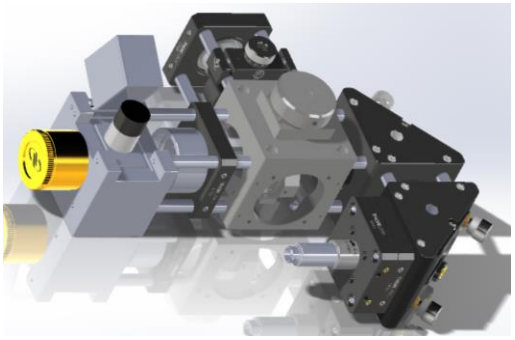

III. Optical Design Details

The optical block diagram is seen below to demonstrate how the design for all the optics is set up. It starts with light emitting from the laser and hitting each optical component on the way, we can see the input beam path in yellow and output beam path in orange.

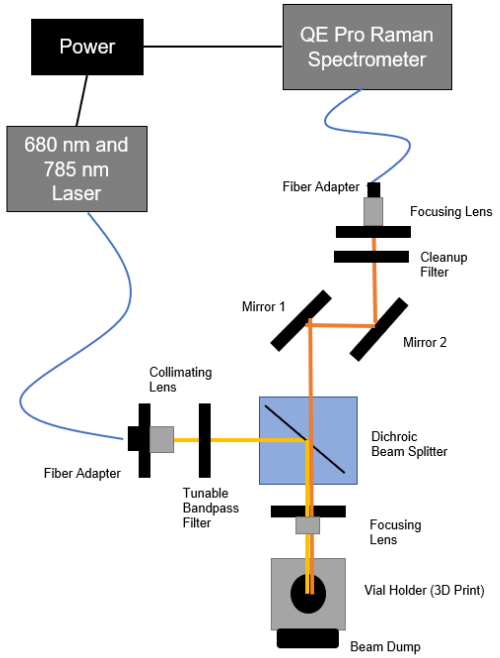

We decided to go with a cage mounting system for ease of use when building and the rods to make sure that everything in the system is always on the same optical plane. Using the cage system with rods as seen in the image below also saves us money and size, as the other option would be to build this system on an optical breadboard. As seen below the image of the optical components in a caged system.

A. *Design of the Optical Lens System*

The RSCL optical design uses filters, fibers, and lenses. From our total afocal optical system, we have an input beam and an output beam. Looking onto the optical beam diagram in figure 3 we can see that the input beam path in yellow on the diagram, starts at the "laser in" fiber end which is connected to a collimating lens. The collimated light goes into the beam splitter and is reflected from the beam splitter turning the beam 90 degrees into the focusing lens and focused onto the sample. The output beam as seen in orange starts with the light that is scattered and reflected from the vial; this beam will go through the previous focusing lens but in reverse producing a collimated beam. This collimated beam will transmit through the beam splitter onto the alignment mirrors and into another focusing lens and the spectrometer fiber end. It was possible to create a ray trace for each of these paths using Zemax. Ignoring the beam splitter and mirrors for these diagrams as they are arbitrary for what we are evaluating the lenses for.

<u>Input Beam Path</u>

The goal with this input beam path (as seen in yellow on the optical diagram) is to focus the beam spot to fall in the middle of the vial. Doing this will eliminate the effect of the vial curvature on the focus. We also want the highest efficiency from the beam onto the focus, this will help the output beam path for the return light to go into the spectrometer fiber. The layout of the collimator (TC18FC-780) to the sample focal point into the vial is as seen below. For this focus onto the vial, we are using an achromatic doublet (AC254-030-B-ML) with a focal length of 30 mm. This 30mm lens' focal length was chosen because we have a restriction on the aperture of 10 mm from the input fiber. The goal here is to have a smaller F#, this will allow more light can be collected and providing a smaller depth of field than a larger F#, which is what we are looking for in our application as we want the focus to stay within the vial. It is easy to see on the layout the entrance aperture isn't the size of the focusing lens, it is the size of the collimating lens as it is smaller which is what the F# is based on. I have the focus

thickness set to be the same as the output layout where the object thickness is the perfect length to have the doublet collimate when the light is reflected from the vial.

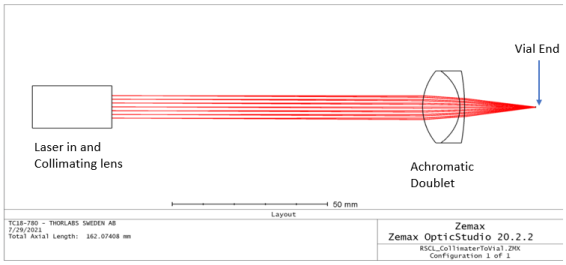

Using the equation below we can calculate that with the aperture diameter of 10 mm and the focal length of 30 mm we get an F# of 3. The 30 mm focal length provides enough working distance from the vial and the vial holder at the smallest F# we could have.

$$\mathrm{F}(\#) = \frac{focal\ length}{entrance\ pupil} \qquad (2)$$

From equation 2, we are seeing the paraxial magnification for this system. In the image below we can see the spot size diagram with an object height of 0.1 mm and at the image we get the chief ray height at -0.168 mm we see that the magnification here is 1.68.

$$mag = \frac{image\ height}{object\ height} = \frac{object\ angle}{image\ angle} \qquad (3)$$

We are also looking at the efficiency at the focus spot on the vial. We can see in the image below we are achieving the goal of high efficiency at 100%. This also tells us that the spot size at the focus is about 0.32 mm. This is a good size as it is a small percentage of the diameter of our 15 mm diameter vials, but it is much larger than a water molecule. On average a water molecule is about 0.27 nm. This means that we have big enough of spot size to test the homogenous samples but small enough that we are not running into any problems with the vial.

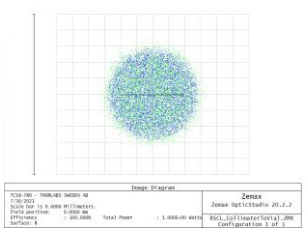

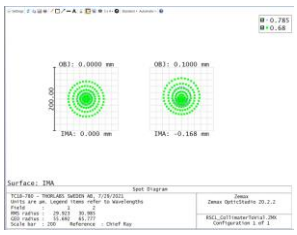

Output Beam Path

The goal through the output path (as seen in orange on the optical diagram) is to receive as much of the beam as possible into the spectrometer fiber tip with the lenses. This fiber (M91L01) is a 0.22 NA, 200 µm fiber with an FC/PC end that directly attaches to a focusing lens to help focus the scattered light. This fixed focus lens (F280FC-850) has a focal length of 18.45 mm and an NA of 0.15. In the figure below we see the focus spot on the left is where the vial will be and it will pass through the achromatic doublet backward, which will cause the beam to collimate. The beam will be refocused by the fiber focusing lens onto the fiber, which is imaged to the right.

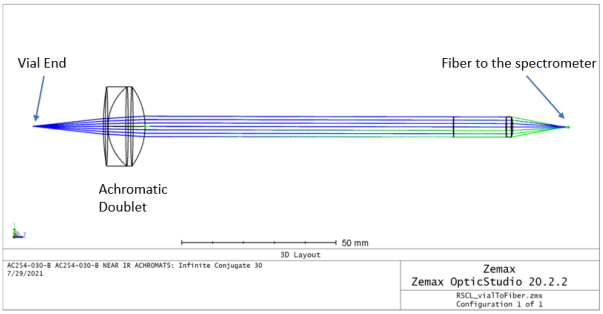

Through Zemax we can image the beam and do a fiber coupling analysis. In the figure below we can see that the fiber coupling efficiency is at 50%. Given the power of the light source and the sensitivity of the detector, this was sufficient for the application. This figure also shows the diameter of the beam and that it corresponds to the 200-um fiber we are using. There is also a spot size diagram for the image plane, this tells us how our spot looks according to wavelength and the paraxial magnification. As seen in the image below, the diameter of the spot is still 200 um and the paraxial magnification shows the image height is -0.011 mm at the image from the 0.1 degrees at the object coming in. We can do a chief ray trace for this paraxial magnification and the equation 3. The magnification here is 1.1.

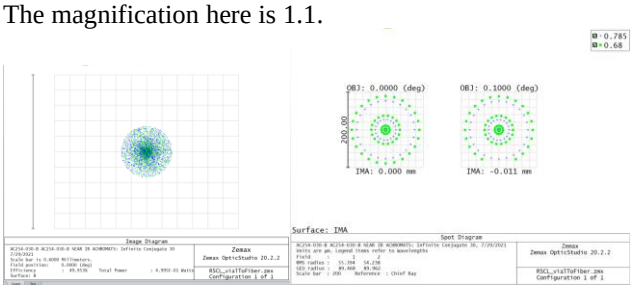

B. *Design of Optical Filters*

When looking at filters for this system we must first understand the principle of Raman spectroscopy, scattered light is a very small percentage of the light going through the system. The scattered light used for Raman through vibrational spectroscopy is about 1 in 10,000 photons. To allow more scattered light to come through the system to provide useful data we can set the integration time to be longer than normal spectroscopy like 1 or 2 seconds compared to milliseconds or

microseconds. Another option that can be used in conjunction with the longer integration time is to use a higher laser power, this means that much of the original wavelength still comes through the system and saturates our spectrometer. To mitigate this, we use filters to help see the weak Raman signal while filtering out the overpowering incident light.

The filters used in this system are to knock down the incident wavelengths, this allows just the scattered light to show and provides much cleaner data. In this project, it is not only about filtering out one wavelength, but it must also block two while allowing the scattered light to pass. The scattered light data for both the incident wavelengths (680 nm and 785 nm) is over 790 nm. This means the stretch region when not Raman shifted is in the same wavelength range as the fingerprint region. This is convenient when looking at filters for the system. To take down the incident wavelengths that are overpowering the spectrometer we can look through the optical diagram at each of the filters seen below.

Tunable Bandpass

Starting at the laser input of the optical system right after the laser in the collimation lens there is a tunable bandpass filter. This Semrock Versa Chrome tunable bandpass filter (TBP01-790) creates a bandpass filter to allow light right around 785 nm to transmit. It is "tunable" because when rotated the bandpass will change its transmission wavelength range. When set to 19 degrees of rotation we see the transmission as seen below. This filter was added later after seeing that we were saturating the spectrum right at the range of 786 nm to 796nm. This is most likely due to the laser having a larger linewidth and emitting higher wavelengths than 785 nm. This filter helps clean up the incident wavelength through to the sample, so the output beam is only from the sample and not a reflection of the higher wavelengths coming from the laser. Below is the Semrock "my light" tool that allows a demonstration of their filters in action, here we can see the angle of incidence is set.

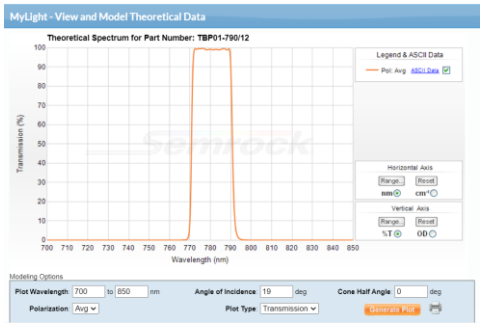

Dichroic Beam Splitter

Right after the tunable bandpass filter, there is the 785nm RazorEdge dichroic laser beam splitter (LPD02-785RU), which allows for Transmission of all wavelengths above 786 nm, and it reflects 680 nm and 785 nm incident wavelengths. This is exactly what we want to help reflect and cut down the incident wavelengths post sample on the system while allowing the scatter light through. We can see this in the figure below keeping in mind that the graph is showing the transmission and the reflection graph would be the inverse of this one. However, this filter alone cannot do all the filtering for the system as the laser is very powerful and this beam splitter can only take down so much, therefore we need a third filter.

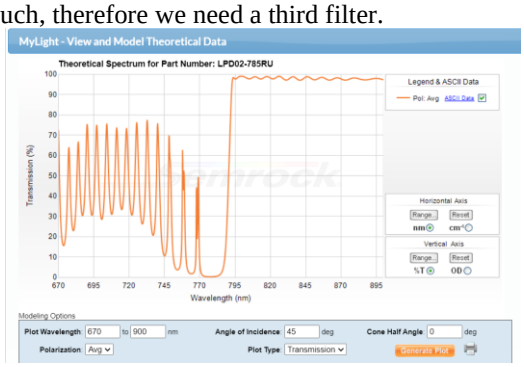

Long Pass Filter

At the end of the system right before the spectrometer fiber focusing lens, there is a Semrock 780 nm RazorEdge® ultra-steep long-pass edge filter (LP02-780RU-25). This is here to cut down the incident laser light once again and only allow the scattered light through. There is a lot of laser light relative to the Raman signal, so we clean it up even more with the long pass filter at the end. We can see the transmission graph of this long pass filter below.

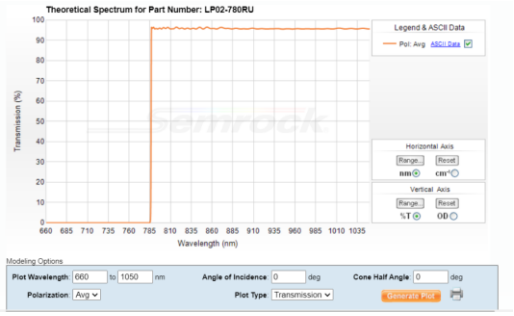

Building the system

Once everything was installed on rods, we just needed to align the system. Through the process of building and testing with the RSCL, we found a couple of minor setbacks. The first vials used created an etaloning with the data because the glass of the vial was most likely coated in something causing a sort of refraction inside of the sample. The other problem was that the 785 nm laser started burning through our thick 3D printed vial holder,

so we implemented a beam dump to catch the residual light as seen in gold in the picture above.

The final iteration of the RSCL is now in a pelican case with only the vial holder cap accessible as well as the laser front and spectrometer. The LattePanda screen is a touch screen to make it quick and easy to take samples.

IV. Hardware/Software Interactions

Moving into the software side of the design, we begin to look at the way the software design interacts with the hardware. There are two main points that this kind of interaction needs to be considered. The development system on the chipboard is used to hold the software prototype, and the drivers to communicate with the QEPro spectrometer.

While many development boards such as the Raspberry Pi Zero and the AML-S905C-CC were considered, the development engineers decided to go with the LattePanda Alpha. This was due to the lack of computing power or software flexibility that other boards offered for the design. These issues were carefully considered during the design process, and it was determined that the LattePanda would offer the smoothest design experience. The presence of Windows 10 already loaded onto the board, and more computing power than would be needed at any point during the design and testing process made it a natural fit into the overall design.

With a development board picked out, the software design can begin to take root. The first portion of the software flow is the drivers which communicate with the QEPro to obtain a spectrum. These drivers are a derivative of Ocean Insight's OceanDirect SDK, which offered utilities that eased the process of communicating with the device itself. These were used to first secure a connection with the spectrometer, check for any errors with the device being entered into the program space, and then capture spectral data to be processed by the rest of the software design. The driver code automatically turns this data into a comma-separated values file format for ease of data manipulation. The driver programs were written in C-Sharp which allows for an easily readable experience for anyone revisiting the code later.

V. Graphical User Interface Design

With a way to communicate with the spectrometer, we need a way for someone to be able to tell the designer what to do and when. A graphical user interface seemed to be the best solution, as it gives the user a way to interact with the design with only a fundamental amount of knowledge of the topics needed, while also limiting their ability to cause errors in the design itself by keeping certain features locked at certain times.

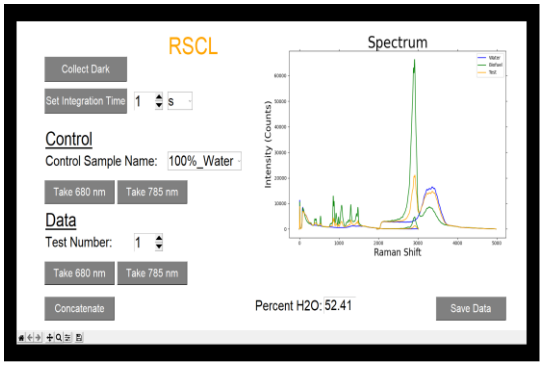

The design consists of multiple buttons, drops downs, and the central focus, a graph to display the collected spectral data. The user can collect dark spectral data to correct errors in the actual control and test samples, as well as increase the integration time to take in more or less light. The integration time can be compared to the shutter on a camera, with the time being the shutter speed, at a longer interval more light will come in causing a more detailed image. The collect dark button must be used first before taking control samples or test samples, as the error correction is required for the rest of the spectral data. Trying to capture other spectral data aside from dark spectral data will cause an error message to be thrown at the user. This is also the point that the software design checks to make sure the spectrometer is correctly connected and taking data normally.

Following this, the user can then take four control samples, two controls with two lasers. This data is then shown on the graph portion of the interface so the user can verify nothing is wrong with the lasers or the sample itself. There is also a blocking mechanism here that prevents the user from taking the test samples. Once all four control samples have been taken, the block is lifted, and the user can take their test samples. The device can collect a theoretically infinite number of samples however the current max is 100, which is far more than necessary. With the test, the sample collected the user can then concatenate the data, with another blocking mechanism here to prevent the user from trying to concatenate too early.

Once all the data has been collected, with a minimum of six scans being taken, the user can concatenate the data onto the graph to show where the two controls and their test sample lie. The sample data should be somewhere in between the two control graphs if the sample is made up of only the two solutions in the control samples. This fact allows for the data analysis to be able to determine an estimation as to what percentage of water the test sample is contaminated with.

Lastly, the user is given the option to save the data collected, which will save the time-stamped data to a folder for use later. This folder with be created if it isn't already present. After the user interface program is stopped, all unsaved data will be deleted. This is to make sure no data is accidentally reused at a later use of the device.

VI. Automation of the Design

To make the software design as smooth for the user as possible, there was a significant aim to automate as much of the design as possible, to limit necessary interaction with the user. The design uses a combination of a batch file and the windows task scheduler to run the graphical user interface on the start-up of the device. The Latte Panda itself also powers on and begins loading into windows within seconds of being connected to the power supply. This is all done so the user doesn't have to worry about managing these portions of the design themselves, they can just plug and play. There was a consideration to completely lock down the unit so the user wouldn't have access to any other portions of the computer aside from the graphical user interface. However, there became a need for the integration time section of the interface to allow the user to enter numeric values using the touch screen keyboard, which can only be accessed from the Windows taskbar. This can be changed in future iterations of the design when future designers determine the best way to input this information, or native step scaling becomes a part of the Python graphical user interface library. The process of determining the percentage of water contamination is also automated for the user, by using a regression line formula calculated in the data analysis section of the design. This allows the user to get an estimate that is at the very least 80% accurate to the actual amount of contamination, with the average estimate being in the 90-95% range.

VII. Data Analysis

With data collected by the first portions of the graphical user interface, the user now can obtain probably the most important information in the design, the estimated water contamination in the fuel sample. To determine this, we needed the formula to be able to calculate a percentage based on previous data and tests.

To begin this process, we collected a series of data ranging from 0% water to 100% water, incrementing the percent contaminant by 3.125% for each data set. From this data and concatenating and analyzing the plotted graphs, one can see that the data values will always fall between our two controls (100% water and 100% biofuel) within the range of approximately 850 nm and 900 nm. Using this information, we took maximum values at this range from each of the data sets, and assigned them key pair values, with an "x" value being the intensity count value, and the "y" value is the percent value associated with that maximum. We were then able to take this data and find a trendline using regression analysis. For this stage, we used the Sci-Kit regression fit tool, which allows us to automatically break down our data sets into train and test data to improve the accuracy of our analysis. This allows us to find the coefficients for our "y = m * x + b" regression line.

The coefficients alone are enough to gather an estimate, but to verify our accuracy and error margins we took the analysis a step further to check our error margins and generate a confidence interval. We then took the values of the coefficients and placed them into the user interface to take in the maximum intensity at the range of 850 nm to 900 nm and use it as an x value in our slope line formula. This generates a y value which is our prediction of the percent contaminant of the unknown test sample. This estimate is at least 80% accurate however with each iteration of the algorithm as well as the addition of data, the error margins will continue to shrink.

For this analysis, we used control samples of pure water and pure biofuel, however, the entire analysis could be redone with any sample that is completely soluble with water. At this point, one can just take new data samples,

and enter them into the analysis program. This program is made to be able to take in data automatically as long as it uses a particular naming convention.

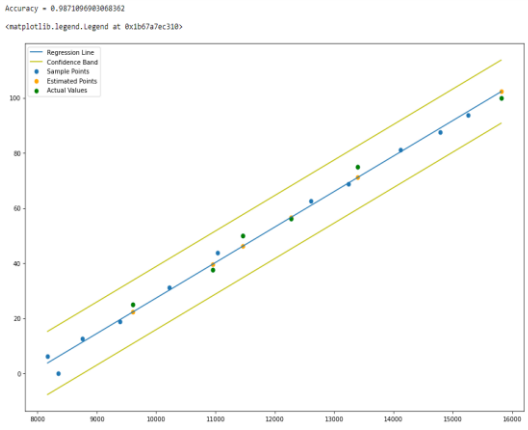

VIII. Bug Testing and Error Correction

During any software design process, there needs to be a testing phase to find any bugs and errors in the code and design. Much of the testing for this design went into the data analysis, to determine the best way to find an accurate estimate, how to use the minor machine learning elements, and what impacts our data negatively. To give an example of the data being impacted, we found that the ambient light of a room was different enough from the lighting in a lab environment that the data taken from a room became completely unusable. This is because the intensity values are affected enough by this outside lighting change to influence the data process. To fix this issue, we took data with our final design, which has much more dark control than a room with large windows or working from a computer screen in a dark lab.

Aside from the data analysis, a significant amount of time went into testing the graphical user interface and finding points that the device could crash or produce unwanted results. For example, there originally were not any checks to verify the user had taken required measurements previously, so the user could attempt to concatenate data without enough data present, which would crash the system. Another instance was the lack of a check that could verify a spectrometer was connected and properly working. Solving this issue, which we implemented into the dark spectrum gathering phase, lead us to discover the graphical user interface could potentially use old data, which would cause results to be skewed. This led to us implementing a mechanism to delete data upon closing the interface, and an option to save data to an isolated area in the program space.

IX. DESIGN CONSTRAINTS AND STANDARDS

The biggest constraint optically is the safety of the laser system. We are using a class 3B high-powered laser. Where beam hazards are potential injury to the eye and potential injury to the skin. Non-Beam hazards include electrocution, fire, exposure to air contaminants, hazardous gases, laser dyes, and solvents. To avoid these hazards, they have implied that these lasers must be in protective housing, warning signs, and label requirements. We would have solved this by using a cap for the vial holder that is connected to an interlock circuit to shut the laser down if the cap is open

X. Conclusion

The purpose of this project is to create an efficient way to find water in fuel and later more chemicals. Although our world is moving towards battery-powered systems in a way to eliminate fuel and pollution, we still use fuel a lot and it will not be replaced that quickly especially for large heavy machinery and equipment. The RSCL will help with the environmentally friendly movement by not letting fuel go to waste and in turn saving engines. If we can check the storage tanks more often it is likely that we can save the fuel before it goes bad or find a way to reverse the damage. As well as always being prepared for natural disaster relief.

We wanted to do this project because it not only challenged everyone in the team to do stretch our field into something, we are not normally used to but also make a system that is not available to markets yet. This project is not only improving Raman Spectroscopy, but it will also guide a new path for water detection systems.

Acknowledgment

The authors wish to acknowledge the amazing sponsorships from Ocean Insight and Innovative Photonic Solutions.

The Engineers

Yaelle Olivier is a 23 year old graduating Optics and Photonics Engineering student who is lined up for a job at Ocean Insight in Orlando, FL to work more with spectroscopy systems.

Tyler is a graduating senior in Computer Engineering: VLSI Circuits. He mainly focuses in Automation, Machine Learning, and VLSI design and security. He was worked at Medline Industries as an Automation Engineer, and Ocean Insight as a Software Engineer. He hopes to go into the industry to use his skills to drive the world forward.

REFERENCES

Software References

[1] "AML-S905X-CC (Le Potato)," *Libre Computer*, 26-Jun-2018. [Online]. Available: https://libre.computer/products/boards/aml-s905x-cc/. [Accessed: 23-Apr-2021].

[2] "Autorun a Python script on windows startup," *GeeksforGeeks*, 26-Feb-2019. [Online]. Available: https://www.geeksforgeeks.org/autorun-a-python-script-on-windows-startup/. [Accessed: 23-Apr-2021].

[3] "The C++ Resources Network," *cplusplus.com*. [Online]. Available: https://www.cplusplus.com/. [Accessed: 23-Apr-2021].

[4] "Coding Standards For Quality and Compliance," *Perforce*. [Online]. Available: https://www.perforce.com/resources/qac/coding-standards. [Accessed: 23-Apr-2021].

[5] "Community," *Chocolatey Software*. [Online]. Available: https://community.chocolatey.org/. [Accessed: 23-Apr-2021].

[6] Corob-Msft, "Build and run a C++ console app project," *Microsoft Docs*. [Online]. Available: https://docs.microsoft.com/en-us/cpp/build/vscpp-step-2-build?view=msvc-160. [Accessed: 23-Apr-2021].

[7] Dev Ed, "Build A Python GUI App Tutorial," *YouTube*, 19-Oct-2019. [Online]. Available: https://www.youtube.com/watch?v=jE-SpRI3K5g. [Accessed: 23-Apr-2021].

[8] "Enterprise Open Source and Linux," *Ubuntu*. [Online]. Available: https://ubuntu.com/. [Accessed: 23-Apr-2021].

[9] *GIMP*. [Online]. Available: https://www.gimp.org/. [Accessed: 23-Apr-2021].

[10] J. R. Jacob, "How to make Windows 10 Toast Notifications with Python," *Medium*, 26-Jan-2018. [Online]. Available: https://towardsdatascience.com/how-to-make-windows-10-toast-notifications-with-python-fb3c27ae45b9. [Accessed: 23-Apr-2021].

[11] *java.com*. [Online]. Available: https://www.java.com/en/download/manual.jsp. [Accessed: 23-Apr-2021].

[12] K. Foundation, "Digital Painting. Creative Freedom.," *Krita*, 31-Aug-2020. [Online]. Available: https://krita.org/en/. [Accessed: 23-Apr-2021].

[13] "LattePanda Delta 432 – Tiny Ultimate Windows / Linux Device 4GB/32GB," *DFRobot*. [Online]. Available: https://www.dfrobot.com/product-1908.html. [Accessed: 23-Apr-2021].

[14] "LattePanda Delta 432," *LattePanda*. [Online]. Available: https://www.lattepanda.com/products/lattepanda-delta-432.html. [Accessed: 23-Apr-2021].

[15] "Libre Computer Board AML-S905X-CC (Le Potato) 2GB 64-bit Mini Computer for 4K Media," *Amazon*. [Online]. Available: https://www.amazon.com/Libre-Computer-AML-S905X-CC-Potato-64-bit/dp/B074P6BNGZ/ref=sr_1_1?dchild=1&keywords=%22libre+computer%22+aml-s905x-cc&linkCode=sl2&linkId=6ef3196e613636af4f5bb7dfcd2d9935&qid=1619204469&sr=8-1. [Accessed: 23-Apr-2021].

[16] M. Huculak, "Running your first batch script on Windows 10," *Windows Central*, 16-Oct-2020. [Online]. Available: https://www.windowscentral.com/how-create-and-run-batch-file-windows-10. [Accessed: 23-Apr-2021].

[17] "Microsoft Windows 10 Home | Download," *Amazon*. [Online]. Available: https://www.amazon.com/Microsoft-Windows-10-Home-Download/dp/B01019BM7O/ref=sr_1_3?dchild=1&keywords=windows+10&qid=1619204726&sr=8-3. [Accessed: 23-Apr-2021].

[18] "Microsoft," *Microsoft Support*. [Online]. Available: https://support.microsoft.com/en-us/windows/how-to-open-registry-editor-in-windows-10-deab38e6-91d6-e0aa-4b7c-8878d9e07b11. [Accessed: 23-Apr-2021].

[19] *MyPaint*. [Online]. Available: http://mypaint.org/. [Accessed: 23-Apr-2021].

[20] "OmniDriver and SPAM," *OmniDriver & Spam | Ocean Insight*. [Online]. Available: https://www.oceaninsight.com/products/software/drivers/omnidriver-and-spam/. [Accessed: 23-Apr-2021].

[21] "os - Miscellaneous operating system interfaces," *os - Miscellaneous operating system interfaces - Python 3.9.4 documentation*. [Online]. Available: https://docs.python.org/3/library/os.html. [Accessed: 23-Apr-2021].

[22] *Project Jupyter*. [Online]. Available: https://jupyter.org/. [Accessed: 23-Apr-2021].

[23] "PyCharm: the Python IDE for Professional Developers by JetBrains," *JetBrains*. [Online]. Available: https://www.jetbrains.com/pycharm/. [Accessed: 23-Apr-2021].

[24] "Python 3.0 Release," *Python.org*. [Online]. Available: https://www.python.org/download/releases/3.0/. [Accessed: 23-Apr-2021].

[25] Raspberry Pi, "Buy a Raspberry Pi Zero W," *Raspberry Pi*. [Online]. Available: https://www.raspberrypi.org/products/raspberry-pi-zero-w/. [Accessed: 23-Apr-2021].

[26] S. Brink, "Add VBScript File to New Context Menu in Windows 10," *Windows 10 Help Forums RSS*, 30-May-2020. [Online]. Available: https://www.tenforums.com/tutorials/8011-add-vbscript-file-new-context-menu-windows-10-a.html#:~:text=A%20.,vb%20file%20extension. [Accessed: 23-Apr-2021].

[27] S. Team, *Home - Spyder IDE*. [Online]. Available: https://www.spyder-ide.org/. [Accessed: 23-Apr-2021].

[28] "seabreeze," *python*. [Online]. Available: https://python-seabreeze.readthedocs.io/en/latest/. [Accessed: 23-Apr-2021].

[29] T. Scott, "FizzBuzz: One Simple Interview Question," *YouTube*, 31-Jul-2017. [Online]. Available: https://www.youtube.com/watch?v=QPZ0pIK_wsc. [Accessed: 23-Apr-2021].

[30] "tkinter - Python interface to Tcl/Tk," *tkinter - Python interface to Tcl/Tk - Python 3.9.4 documentation*. [Online]. Available: https://docs.python.org/3/library/tkinter.html. [Accessed: 23-Apr-2021].

[31] "Visual Studio IDE, Code Editor, Azure DevOps, & App Center," *Visual Studio*, 22-Apr-2021. [Online]. Available: https://visualstudio.microsoft.com/. [Accessed: 23-Apr-2021].

[32] W. Gay, "Advanced Raspberry Pi: Raspbian Linux and GPIO Integration," *Amazon*, 2018. [Online]. Available: https://www.amazon.com/Raspberry-Pi-Zero-Wireless-model/dp/B06XFZC3BX. [Accessed: 23-Apr-2021].

[33] "win10toast," *PyPI*. [Online]. Available: https://pypi.org/project/win10toast/. [Accessed: 23-Apr-2021].

[34] "The World's Most Popular Data Science Platform," *Anaconda*. [Online]. Available: https://www.anaconda.com/. [Accessed: 23-Apr-2021].

Optical References

[35] "ANSI Z136.1 - Safe Use of Lasers," *The Laser Institute*, 08-Oct-2020. [Online]. Available: https://www.lia.org/resources/laser-safety-information/laser-safety-standards/ansi-z136-standards/z136-1. [Accessed: 27-Apr-2021].

[36] B. Performance, "Fuel additives: Diesel additives: Oil additives: Bell performance." [Online]. Available: https://www.bellperformance.com/. [Accessed: 26-Apr-2021].

[37] By: Chad Christiansen Product Quality and Additives Manager in Agriculture and Farming and C. Christiansen, "Warning signs your diesel is water-contaminated." [Online]. Available: https://www.cenex.com/about/cenex-information/cenexperts-blog-page/agriculture-and-farming/water-contaminated-diesel. [Accessed: 26-Apr-2021].

[38] Center for Devices and Radiological Health, "Important Information for Laser Pointer Manufacturers," *U.S. Food and Drug Administration*. [Online]. Available: https://www.fda.gov/radiation-emitting-products/laser-products-and-instruments/important-information-laser-pointer-manufacturers. [Accessed: 27-Apr-2021].

[39] Center for Devices and Radiological Health, "Laser Products Guidance - IEC 60825-1 Ed. 3 and IEC 60601-2-22 Ed. 3.1," *U.S. Food and Drug Administration*. [Online]. Available: https://www.fda.gov/regulatory-information/search-fda-guidance-documents/laser-products-conformance-iec-60825-1-ed-3-and-iec-60601-2-22-ed-31-laser-notice-no-56. [Accessed: 27-Apr-2021].

[40] "Characterization of gasoline BY Raman spectroscopy with Chemometric analysis." [Online]. Available: https://www.tandfonline.com/doi/abs/10.1080/00032719.2016.1210616. [Accessed: 27-Apr-2021].

[41] H. Ge, Z. Ye, and R. He, "Raman spectroscopy of diesel and gasoline engine-out Soot using different laser power," *Journal of Environmental Sciences*, vol. 79, pp. 74–80, 2019.

[42] J. Kiefer, "Dual-Wavelength Raman Fusion Spectroscopy," *Analytical Chemistry*, vol. 91, no. 3, pp. 1764–1767, 2019.

[43] J. Kiefer, "Dual-Wavelength Raman Spectroscopy: Improved Compactness and Spectral Resolution," *American Pharmaceutical Review*, Oct. 2014.

[44] J. Tedesco, "785-nm laser benefits Raman spectroscopy," 01-Sep-2000. [Online]. Available: https://www.laserfocusworld.com/test-measurement/test-measurement/article/16555494/785nm-laser-benefits-raman-spectroscopy. [Accessed: 27-Apr-2021].

[45] J. Wei, A. Wang, and K. Connor, "COMPARING RAMAN SIGNAL STRENGTHS OF BIOMARKERS AND MINERALS MEASURED BY A MULTI-WAVELENGTH RAMAN SYSTEM ," *Lunar and Planetary Science Conference*, no. 46.

[46] L. T. Kerr, H. J. Byrne, and B. M. Hennelly, "Optimal choice of sample substrate and laser wavelength for Raman spectroscopic analysis of biological specimen," *Analytical Methods*, vol. 7, no. 12, pp. 5041–5052, 2015.

[47] M. P. Arroyo, T. P. Birbeck, D. S. Baer, and R. K. Hanson, "Dual diode-laser fiber-optic diagnostic for water-vapor measurements," *Optics Letters*, vol. 19, no. 14, p. 1091, 1994.

[48] M. T. Meyer, "How Does Concatenation Enhance Raman Spectroscopy?," *RPMC Lasers Blog*. [Online]. Available: https://blog.rpmclasers.com/how-does-concatenation-enhance-raman-spectroscopy. [Accessed: 27-Apr-2021].

[49] P. Edmonds and J. J. Cooney, "Identification of Microorganisms isolated from jet fuel systems," *Applied Microbiology*, vol. 15, no. 2, pp. 411–416, 1967.

[50] "Raman: Wavelength Matters," *Wasatch Photonics*, 16-Jun-2020. [Online]. Available: https://wasatchphotonics.com/technologies/raman-spectroscopy-wavelength-matters/. [Accessed: 27-Apr-2021].

[51] *RamanBasics*. [Online]. Available: https://www.sas.upenn.edu/~crulli/RamanBasics.html. [Accessed: 27-Apr-2021].

[52] Source, "New, less-expensive testing Method approved for Containment Sumps," 01-Jun-2017. [Online]. Available: https://www.sourcena.com/sourceline/new-less-expensive-testing-method-approved-containment-sumps/. [Accessed: 26-Apr-2021].

[53] Sponsored by B&W TekJan 25 2021, "Correct laser wavelength for raman material identification," 25-Jan-2021. [Online]. Available: https://www.azom.com/article.aspx?ArticleID=11871. [Accessed: 27-Apr-2021].

[54] T. Hill, "Microbial growth in aviation fuel," *Aircraft Engineering and Aerospace Technology*, vol. 75, no. 5, pp. 497–502, 2003.

[55] T. Hill, "Microbial growth in aviation fuel," *Aircraft Engineering and Aerospace Technology*, vol. 75, no. 5, pp. 497–502, 2003.

[56] Y. Mattley, “Characterization of Diesel Fuel Using a Modular Raman System,” *Spectroscopy -Springfield then Eugene then Duluth-* , vol. 29, Dec. 2014.
[57] Z136.2 - Safe Use of Optical Fiber Communication Systems Utilizing Laser Diode and LED Sources,” *The Laser Institute*, 29-Aug-2017. [Online]. Available: https://www.lia.org/resources/laser-safety-information/laser-safety-standards/ansi-z136-standards/z136-2. [Accessed: 27-Apr-2021].